

Teleporting an unknown quantum state to a photon with prior quantum information

Tianfeng Feng,^{1,*} Qiao Xu,^{1,*} Linxiang Zhou,^{1,*} Maolin Luo,¹ Wuhong Zhang,^{1,2} and Xiaoqi Zhou^{1,†}

¹*State Key Laboratory of Optoelectronic Materials and Technologies and School of Physics,
Sun Yat-sen University, Guangzhou, People's Republic of China*

²*Department of Physics, Jiujiang Research Institute and Collaborative Innovation Center for
Optoelectronic Semiconductors and Efficient Devices, Xiamen University, Xiamen 361005, China*

Quantum teleportation provides a “disembodied” way to transfer an unknown quantum state from one quantum system to another. However, all teleportation experiments to date are limited to cases where the target quantum system contains no prior quantum information. Here we propose a scheme for teleporting a quantum state to a quantum system with prior quantum information. By using an optical qubit-ququart entangling gate, we have experimentally demonstrated the new teleportation protocol—teleporting a qubit to a photon preloaded with one qubit of quantum information. After the teleportation, the target photon contains two qubits of quantum information, one from the teleported qubit and the other from the pre-existing qubit. The teleportation fidelities range from 0.70 to 0.92, all above the classical limit of $2/3$. Our work sheds light on a new direction for quantum teleportation and demonstrates our ability to implement entangling operations beyond two-level quantum systems.

PACS numbers:

Quantum teleportation, a way to faithfully transfer quantum states from one system to another, is one of the most important protocols in quantum information science [1]. Not only is it central to long-distance quantum communication [2] and distributed quantum networks [3], but it also plays a pivotal role in measurement-based quantum computation [4–6]. Quantum teleportation has been experimentally demonstrated in a variety of physical systems, including photons [7, 8], atoms [9], ions [10, 11], electrons [12], defects in solid states [13], and superconducting circuits [14]. Recently, more complex experiments have also been reported, such as the open destination teleportation [15, 16] and the teleportation of a composite system [17], a multi-level state [18, 19], and multi-degree of freedom of a particle [20]. In all of these experiments, the quantum state is transferred from system A, which originally contains all the quantum information, to system B, which is initially either part of an entangled state or in a blank state [7–20] and thus contains no prior information at all. This raises a novel and fundamental question - if system B has been preloaded

with some quantum information beforehand, is it possible to teleport a quantum state from system A to system B without affecting B's pre-existing quantum information. We give a positive answer to this question and present a general scheme to realize this new type of teleportation. By using an optical qubit-ququart entangling gate, we have experimentally teleported a single-qubit quantum state stored in a photon to another photon preloaded with one qubit of quantum information. After the teleportation, the target photon stores two qubits of quantum information, one from the preloaded qubit and the other from the teleported qubit. Besides the fundamental interest, this new teleportation protocol has the potential to simplify the construction of quantum circuits and may find applications in quantum computation and quantum communications.

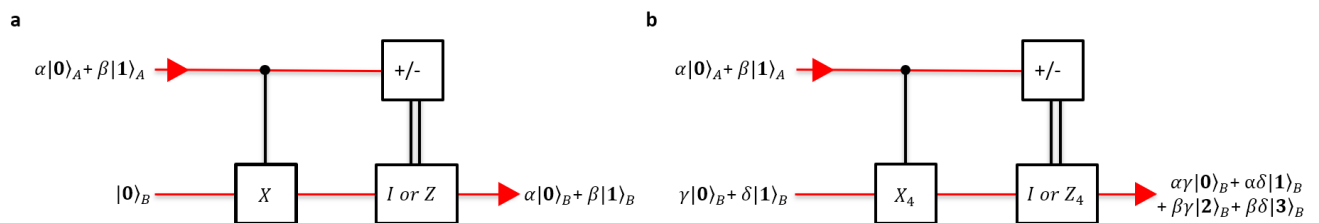


FIG. 1: **Schematic diagrams for local quantum teleportation.** **a**, The standard local quantum teleportation. The CX gate entangles system A, which initially contains one qubit of quantum information, and system B, which initially contains no quantum information. The projective measurement on system A then removes quantum information from A, thus transferring the one qubit of quantum information to B. After the feedforward unitary operation, the quantum state originally stored in A is restored in B, thus completing the standard local quantum teleportation. **b**, The general local quantum teleportation. The initial states of both system A and system B contain one qubit of quantum information. A and B are then entangled by a CX_4 gate, where X_4 converts $|0\rangle$ to $|2\rangle$ and $|1\rangle$ to $|3\rangle$. After the projective measurement and the feedforward unitary operation, the quantum state of A is transferred to B, which now contains two qubits of quantum information.

Local quantum teleportation—Before presenting our new teleportation scheme, we first briefly review the protocol of local quantum teleportation [21, 22]. Unlike the standard quantum teleportation protocol, in the local quantum teleportation protocol, the transfer of quantum states between different systems is achieved through an entangling quantum gate and does not require the use of entangled states as resources. Suppose system A is in the state $\alpha|0\rangle_A + \beta|1\rangle_A$, which contains one qubit of quantum information, and system B is in the blank state $|0\rangle_B$. As shown

in Fig. 1a, by applying a controlled-X gate (CX gate, commonly referred as CNOT gate) on A and B, the quantum state of the composite system of A and B would become

$$\begin{aligned} & \alpha|\mathbf{0}\rangle_A|\mathbf{0}\rangle_B + \beta|\mathbf{1}\rangle_A|\mathbf{1}\rangle_B \\ &= \frac{1}{\sqrt{2}}|+\rangle_A(\alpha|\mathbf{0}\rangle_B + \beta|\mathbf{1}\rangle_B) + \frac{1}{\sqrt{2}}|-\rangle_A(\alpha|\mathbf{0}\rangle_B - \beta|\mathbf{1}\rangle_B), \end{aligned}$$

where $X|\mathbf{0}\rangle = |\mathbf{1}\rangle$, $X|\mathbf{1}\rangle = |\mathbf{0}\rangle$ and $|\pm\rangle = \frac{1}{\sqrt{2}}(|\mathbf{0}\rangle \pm |\mathbf{1}\rangle)$. After measuring A in the $|\pm\rangle$ basis and forwarding the measurement outcome to B, a unitary operation (I or Z) based on the outcome is applied on system B and thus convert its state to $\alpha|\mathbf{0}\rangle_B + \beta|\mathbf{1}\rangle_B$. The state of system B now has the same form as the initial state of system A and thus completes the local quantum teleportation.

General local quantum teleportation—We now present the general local quantum teleportation scheme where the target system can be preloaded with quantum information. While the initial state of system A is still in $\alpha|\mathbf{0}\rangle_A + \beta|\mathbf{1}\rangle_A$, the initial state of system B is now in $\gamma|\mathbf{0}\rangle_B + \delta|\mathbf{1}\rangle_B$, containing one qubit of quantum information. We note that the quantum circuit in Fig. 1a cannot achieve the local quantum teleportation in this case because it keeps system B in a two-dimensional Hilbert space, resulting in its inability to store two qubits of quantum information. To circumvent this problem, the Hilbert space of system B needs to be expanded so that it can carry two qubits of quantum information. As shown in Fig. 1b, a controlled- X_4 gate (CX_4) is applied to A and B, where X_4 is a four-dimensional unitary gate defined as

$$X_4 = \begin{pmatrix} 0 & 0 & 1 & 0 \\ 0 & 0 & 0 & 1 \\ 1 & 0 & 0 & 0 \\ 0 & 1 & 0 & 0 \end{pmatrix},$$

which can convert $|\mathbf{0}\rangle$ to $|\mathbf{2}\rangle$ and $|\mathbf{1}\rangle$ to $|\mathbf{3}\rangle$, expanding the state space of system B from two to four dimensions. The state of A and B is thus converted from

$$\begin{aligned} & (\alpha|\mathbf{0}\rangle_A + \beta|\mathbf{1}\rangle_A) \otimes (\gamma|\mathbf{0}\rangle_B + \delta|\mathbf{1}\rangle_B) \\ &= \alpha\gamma|\mathbf{0}\rangle_A|\mathbf{0}\rangle_B + \alpha\delta|\mathbf{0}\rangle_A|\mathbf{1}\rangle_B + \beta\gamma|\mathbf{1}\rangle_A|\mathbf{0}\rangle_B + \beta\delta|\mathbf{1}\rangle_A|\mathbf{1}\rangle_B \end{aligned} \quad (1)$$

to

$$\begin{aligned} & \alpha\gamma|\mathbf{0}\rangle_A|\mathbf{0}\rangle_B + \alpha\delta|\mathbf{0}\rangle_A|\mathbf{1}\rangle_B + \beta\gamma|\mathbf{1}\rangle_A|\mathbf{2}\rangle_B + \beta\delta|\mathbf{1}\rangle_A|\mathbf{3}\rangle_B \\ &= |+\rangle_A(\alpha\gamma|\mathbf{0}\rangle_B + \alpha\delta|\mathbf{1}\rangle_B + \beta\gamma|\mathbf{2}\rangle_B + \beta\delta|\mathbf{3}\rangle_B) \\ &+ |-\rangle_A(\alpha\gamma|\mathbf{0}\rangle_B + \alpha\delta|\mathbf{1}\rangle_B - \beta\gamma|\mathbf{2}\rangle_B - \beta\delta|\mathbf{3}\rangle_B). \end{aligned}$$

Similarly, after measuring A in the $|\pm\rangle$ basis and forwarding the outcome to B, a four-dimensional unitary operation (I_4 or Z_4) is applied on B conditioned on the outcome and thus converts its state to

$$\alpha\gamma|\mathbf{0}\rangle_B + \alpha\delta|\mathbf{1}\rangle_B + \beta\gamma|\mathbf{2}\rangle_B + \beta\delta|\mathbf{3}\rangle_B, \quad (2)$$

where

$$I_4 = \begin{pmatrix} 1 & 0 & 0 & 0 \\ 0 & 1 & 0 & 0 \\ 0 & 0 & 1 & 0 \\ 0 & 0 & 0 & 1 \end{pmatrix}, \quad Z_4 = \begin{pmatrix} 1 & 0 & 0 & 0 \\ 0 & 1 & 0 & 0 \\ 0 & 0 & -1 & 0 \\ 0 & 0 & 0 & -1 \end{pmatrix}.$$

By comparing Eq. (2) and Eq. (1), it can be seen that the two quantum states have exactly the same form except for the difference in the state basis, which means that the two qubits of quantum information originally stored in A and B are now all stored in system B. In other words, all the quantum information originally stored in A has been transferred to B without affecting the pre-existing quantum information stored in B. We note that the initial state of A and B are chosen as a separable state purely for the convenience of the derivation, and this scheme still holds when the initial state of A and B is entangled.

Optical CX_4 gate—To experimentally implement the general local quantum teleportation scheme described above, the main challenge lies in realizing the key part of the quantum circuit, namely the CX_4 gate, which is a qubit-quart entangling gate. To date, most experimentally realized quantum gates are based on qubits [23–29], and it is a challenging task to implement such high-dimensional entangling operations in any physical system.

Here we present our method of implementing the CX_4 gate in the optical system. As shown in Fig. 2a, instead of implementing the CX_4 gate directly, we first decompose it into two consecutive gates CX_{02} and CX_{13} based on the fact that $X_4 = X_{13}X_{02}$, where

$$X_{02} = \begin{pmatrix} 0 & 0 & 1 & 0 \\ 0 & 1 & 0 & 0 \\ 1 & 0 & 0 & 0 \\ 0 & 0 & 0 & 1 \end{pmatrix}, \quad X_{13} = \begin{pmatrix} 1 & 0 & 0 & 0 \\ 0 & 0 & 0 & 1 \\ 0 & 0 & 1 & 0 \\ 0 & 1 & 0 & 0 \end{pmatrix}.$$

Although X_{02} (X_{13}) is a four-dimensional unitary gate, it only operates on a two-dimensional subspace spanned by $|\mathbf{0}\rangle$ and $|\mathbf{2}\rangle$ ($|\mathbf{1}\rangle$ and $|\mathbf{3}\rangle$). X_{02} (X_{13}) swaps $|\mathbf{0}\rangle$ and $|\mathbf{2}\rangle$ ($|\mathbf{1}\rangle$ and $|\mathbf{3}\rangle$) and leaves $|\mathbf{1}\rangle$ and $|\mathbf{3}\rangle$ ($|\mathbf{0}\rangle$ and $|\mathbf{2}\rangle$) unchanged. Based on this fact, two optical CNOT gates can be used to implement CX_{02} and CX_{13} .

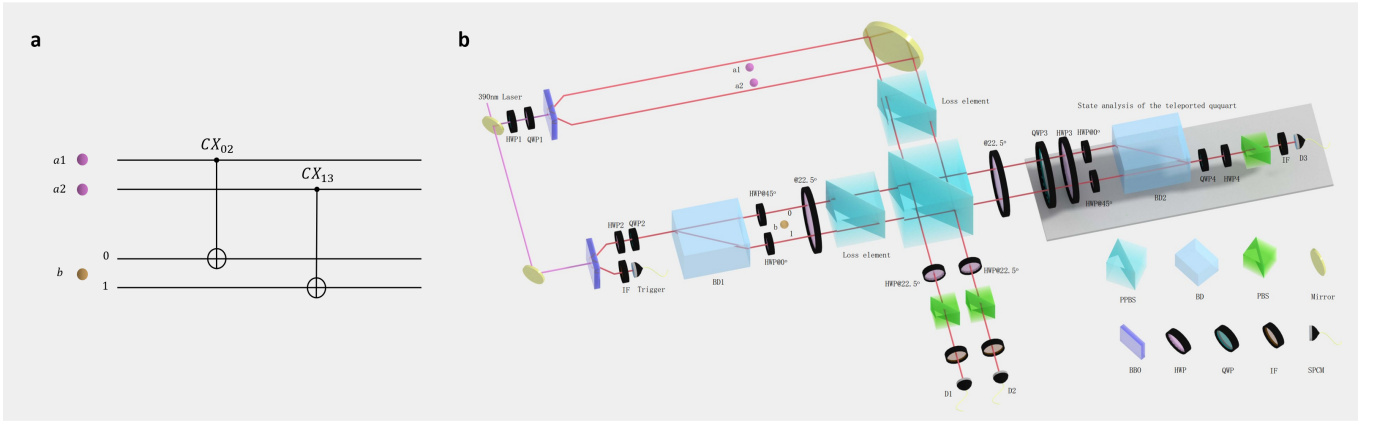


FIG. 2: Experimental layout for general local quantum teleportation. **a**, Optical CX_4 gate. Two photons $a1$ and $a2$ are used to encode qubit A, where $|0\rangle_A = |H\rangle_{a1}|H\rangle_{a2}$ and $|1\rangle_A = |V\rangle_{a1}|V\rangle_{a2}$. Photon b is used to encode ququart B, where $|0\rangle_B = |H0\rangle_b$, $|1\rangle_B = |H1\rangle_b$, $|2\rangle_B = |V0\rangle_b$ and $|3\rangle_B = |V1\rangle_b$. $H0$ ($H1$) denotes photon in the upper (lower) spatial mode with horizontal polarization and $V0$ ($V1$) denotes photon in upper (lower) spatial mode with vertical polarization. A CX_4 gate between the control qubit A and the target ququart B is decomposed into a CX_{02} gate and a CX_{13} gate. The CX_{02} (CX_{13}) gate is equivalent to a polarization CNOT gate operating on photon $a1$ ($a2$) and photon b in the upper (lower) rail. **b**, Experimental setup. A pulsed ultraviolet (UV) laser is focused on two beta-barium borate (BBO) crystals and produces two photon pairs $a1$ - $a2$ and b - t . By tuning HWP1 and QWP1, the first photon pair, $a1$ - $a2$, is prepared at $\alpha|H\rangle_{a1}|H\rangle_{a2} + \beta|V\rangle_{a1}|V\rangle_{a2}$, which serves as the initial state of system A. By tuning HWP2 and QWP2, photon b is prepared at $\gamma|H\rangle_b + \delta|V\rangle_b$. The beam displacer BD1 and its three surrounding HWPs then converts photon b to $\gamma|H0\rangle_b + \delta|H1\rangle_b$, which serves as the initial state of system B. The two polarization CNOT gates based on PPBS are used to implement the optical CX_4 on system A and system B. BD2 and its surrounding waveplates (QWP3, HWP3, HWP@0°, HWP@45°, QWP4 and HWP4) are used to analyze the ququart state.

As shown in Fig. 2a, system A consists of photons $a1$ and $a2$, serving as the control qubit, and system B consists of photon b , serving as the target ququart. The two orthonormal basis states of A are $|0\rangle_A = |H\rangle_{a1}|H\rangle_{a2}$ and $|1\rangle_A = |V\rangle_{a1}|V\rangle_{a2}$, where H (V) denotes horizontal (vertical) polarization. The initial state of qubit A can then be written as $\alpha|0\rangle_A + \beta|1\rangle_A = \alpha|H\rangle_{a1}|H\rangle_{a2} + \beta|V\rangle_{a1}|V\rangle_{a2}$. For system B, to encode a ququart with a single photon b , both the polarization and spatial degree of freedoms are used, and the four orthonormal basis states are $|0\rangle_B = |H0\rangle_b$, $|1\rangle_B = |H1\rangle_b$, $|2\rangle_B = |V0\rangle_b$ and $|3\rangle_B = |V1\rangle_b$, where $H0$ ($H1$) denotes photon in the upper (lower) spatial mode

with horizontal polarization and $V0$ ($V1$) denotes photon in the upper (lower) spatial mode with vertical polarization. The initial state of B can be written as $\gamma|\mathbf{0}\rangle_B + \delta|\mathbf{1}\rangle_B = \gamma|H0\rangle_b + \delta|H1\rangle_b$. The CX_{02} operation between qubit A and ququart B can be realized by applying a polarization CNOT gate to photon a1 and photon b in the upper path, which can be understood as follows: When the polarization of photon a1 is H (namely qubit A in $|\mathbf{0}\rangle_A$), nothing happens; when the polarization of photon a is V (namely qubit A in $|\mathbf{1}\rangle_A$), the polarization of photon b flips between H and V if b is in the upper path (namely ququart B's $|\mathbf{0}\rangle_B$ and $|\mathbf{2}\rangle_B$ components being swapped), and is unaffected if b is in the lower path (namely ququart B's $|\mathbf{1}\rangle_B$ and $|\mathbf{3}\rangle_B$ components being unchanged), which is exactly what a CX_{02} gate achieves. Similarly, the CX_{13} operation can be realized by applying a polarization CNOT gate to photon a2 and photon b in the lower path. As a result, the desired CX_4 gate can be achieved by the two polarization CNOT gates as shown in Fig. 2a.

We note that the reason for using two photons to encode the control qubit is due to the following experimental considerations. The CNOT gates we will use experimentally are based on post-selection measurements, and such CNOT gates would fail when they act twice in a row between the same two photons. By using two photons a1 and a2 to encode the control qubit, the two CNOT gates are not acting between the same two photons, thus avoiding this problem.

Experimental demonstration—Figure 2b shows the experimental setup for the two quantum state transfer schemes. Two photon pairs are generated by passing femtosecond-pulse UV laser through type-II beta-barium borate (BBO) crystals (See Methods: Generating two photon pairs). Photons a1 and a2 of the first pair are prepared at $\alpha|H\rangle_{a1}|H\rangle_{a2} + \beta|V\rangle_{a1}|V\rangle_{a2}$, which serves as the initial state of system A. Photon b from the second pair is prepared at $\gamma|H\rangle_b + \delta|V\rangle_b$. The beam displacer BD1 and its surrounding three half waveplates (two at 45° and one at 0°) are used to expand the Hilbert space of photon b, converting its state to $\gamma|H0\rangle_b + \delta|H1\rangle_b$, which serves as the initial state of system B. The upper (lower) rail of photon b is then superposed with photon a1 (a2) on a partial polarization beamsplitter (PPBS). The PPBS, the loss elements and its surrounding half wave-plates can realize a polarization CNOT gate on photon a1 (a2) and photon b in the upper (lower) path [3]. These two polarization CNOT gates together realize a CX_4 gate on qubit A and ququart B (See Methods: Implementation of CX_4 gate using linear

optics), and the state of the three photons becomes

$$\begin{aligned} & \alpha|H\rangle_{a1}|H\rangle_{a2} \otimes (\gamma|H0\rangle_b + \delta|H1\rangle_b) \\ & + \beta|V\rangle_{a1}|V\rangle_{a2} \otimes (\gamma|V0\rangle_b + \delta|V1\rangle_b). \end{aligned}$$

Active feed-forward is needed for a full, deterministic general local quantum teleportation. However, in this proof-of-principle experiment, we did not apply feed-forward but used post-selection to realize a probabilistic general local quantum teleportation. By projecting both photons a1 and a2 to $|D\rangle = \frac{1}{\sqrt{2}}(|H\rangle + |V\rangle)$, the quantum information of system A (photons a1 and a2) is successfully transferred to system B (photon b), and the state of photon b becomes $\alpha\gamma|H0\rangle_b + \alpha\delta|H1\rangle_b + \beta\gamma|V0\rangle_b + \beta\delta|V1\rangle_b$, which is a ququart state containing two qubits of quantum information.

To demonstrate the validity of our scheme, we have prepared 9 different initial states for teleportation,

$$\begin{aligned} |\psi_1\rangle_{AB} &= \frac{1}{\sqrt{2}}(|\mathbf{0}\rangle_A + i|\mathbf{1}\rangle_A) \otimes |\mathbf{0}\rangle_B \\ &= \frac{1}{\sqrt{2}}(|H\rangle_{a1}|H\rangle_{a2} + i|V\rangle_{a1}|V\rangle_{a2}) \otimes |H0\rangle_b, \\ |\psi_2\rangle_{AB} &= \frac{1}{\sqrt{2}}(|\mathbf{0}\rangle_A + i|\mathbf{1}\rangle_A) \otimes \frac{1}{\sqrt{2}}(|\mathbf{0}\rangle_B - |\mathbf{1}\rangle_B) \\ &= \frac{1}{\sqrt{2}}(|H\rangle_{a1}|H\rangle_{a2} + i|V\rangle_{a1}|V\rangle_{a2}) \otimes \frac{1}{\sqrt{2}}(|H0\rangle_b - |H1\rangle_b), \\ |\psi_3\rangle_{AB} &= \frac{1}{\sqrt{2}}(|\mathbf{0}\rangle_A + i|\mathbf{1}\rangle_A) \otimes \frac{1}{\sqrt{2}}(|\mathbf{0}\rangle_B + i|\mathbf{1}\rangle_B) \\ &= \frac{1}{\sqrt{2}}(|H\rangle_{a1}|H\rangle_{a2} + i|V\rangle_{a1}|V\rangle_{a2}) \otimes \frac{1}{\sqrt{2}}(|H0\rangle_b + i|H1\rangle_b), \\ |\psi_4\rangle_{AB} &= \frac{1}{\sqrt{2}}(|\mathbf{0}\rangle_A + |\mathbf{1}\rangle_A) \otimes |\mathbf{0}\rangle_B \\ &= \frac{1}{\sqrt{2}}(|H\rangle_{a1}|H\rangle_{a2} + |V\rangle_{a1}|V\rangle_{a2}) \otimes |H0\rangle_b, \\ |\psi_5\rangle_{AB} &= \frac{1}{\sqrt{2}}(|\mathbf{0}\rangle_A + |\mathbf{1}\rangle_A) \otimes \frac{1}{\sqrt{2}}(|\mathbf{0}\rangle_B + |\mathbf{1}\rangle_B) \\ &= \frac{1}{\sqrt{2}}(|H\rangle_{a1}|H\rangle_{a2} + |V\rangle_{a1}|V\rangle_{a2}) \otimes \frac{1}{\sqrt{2}}(|H0\rangle_b + |H1\rangle_b), \\ |\psi_6\rangle_{AB} &= \frac{1}{\sqrt{2}}(|\mathbf{0}\rangle_A + |\mathbf{1}\rangle_A) \otimes \frac{1}{\sqrt{2}}(|\mathbf{0}\rangle_B - i|\mathbf{1}\rangle_B) \\ &= \frac{1}{\sqrt{2}}(|H\rangle_{a1}|H\rangle_{a2} + |V\rangle_{a1}|V\rangle_{a2}) \otimes \frac{1}{\sqrt{2}}(|H0\rangle_b - i|H1\rangle_b), \\ |\psi_7\rangle_{AB} &= |\mathbf{1}\rangle_A \otimes |\mathbf{0}\rangle_B = |V\rangle_{a1}|V\rangle_{a2} \otimes |H0\rangle_b, \\ |\psi_8\rangle_{AB} &= |\mathbf{1}\rangle_A \otimes \frac{1}{\sqrt{2}}(|\mathbf{0}\rangle_B + |\mathbf{1}\rangle_B) = |V\rangle_{a1}|V\rangle_{a2} \otimes \frac{1}{\sqrt{2}}(|H0\rangle_b + |H1\rangle_b), \\ |\psi_9\rangle_{AB} &= |\mathbf{1}\rangle_A \otimes \frac{1}{\sqrt{2}}(|\mathbf{0}\rangle_B - i|\mathbf{1}\rangle_B) = |V\rangle_{a1}|V\rangle_{a2} \otimes \frac{1}{\sqrt{2}}(|H0\rangle_b - i|H1\rangle_b). \end{aligned}$$

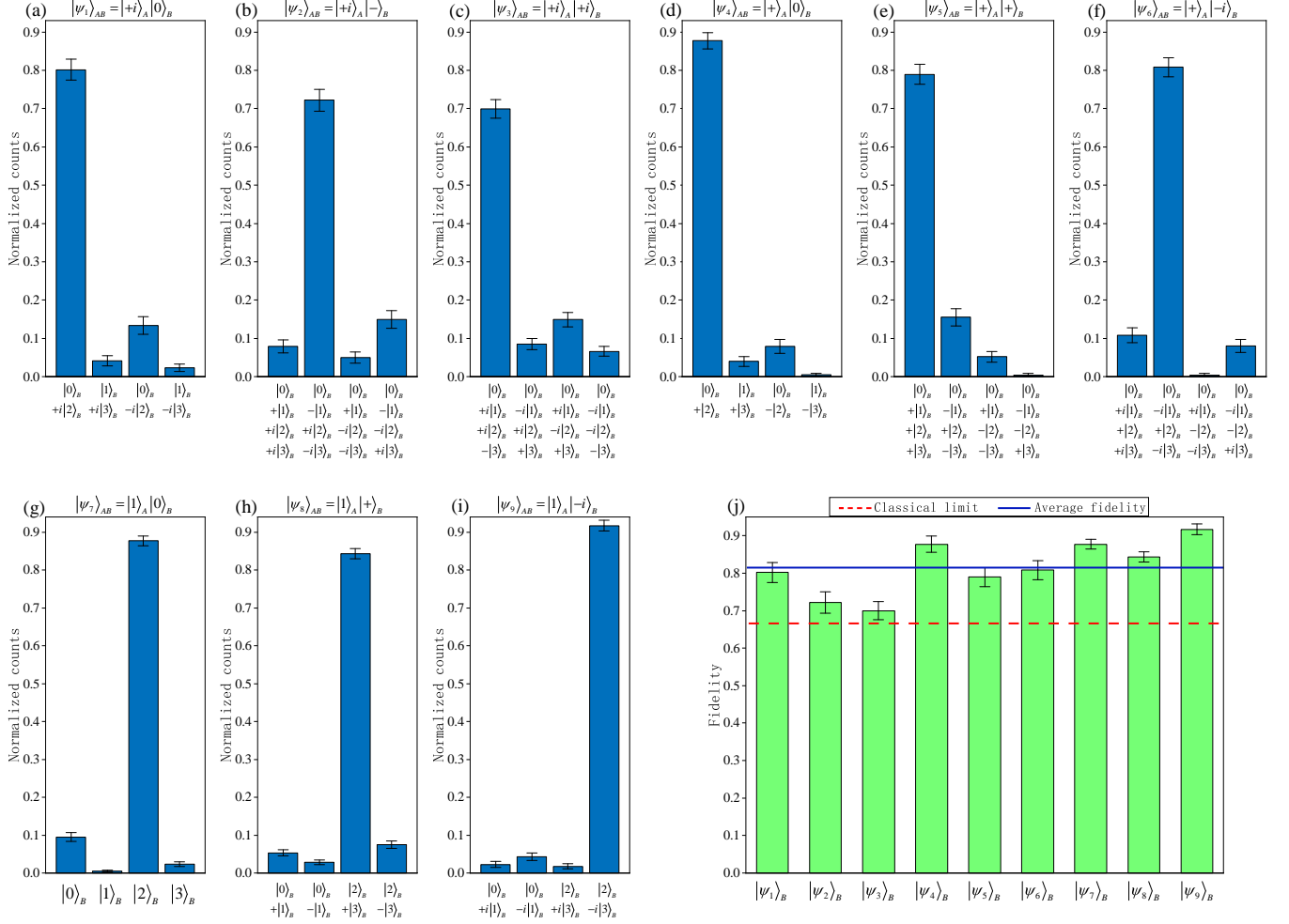


FIG. 3: Experimental results for the general local quantum teleportation. **a-i**, Measurement results of the final state of system B for the initial states $|\psi_1\rangle_{AB}$, $|\psi_2\rangle_{AB}$, ..., and $|\psi_9\rangle_{AB}$. Here $|\pm\rangle = \frac{1}{\sqrt{2}}(|0\rangle \pm |1\rangle)$ and $|\pm i\rangle = \frac{1}{\sqrt{2}}(|0\rangle \pm i|1\rangle)$. **j**, Summary of the fidelities of the general local quantum teleportation for the nine initial states. The average achieved fidelity of 0.8151 ± 0.0074 overcomes the classical bound of $2/3$. The error bars (SD) are calculated according to propagated Poissonian counting statistics of the raw detection events.

After the local teleportation, system B (photon b) should contain all the information of the composite system of A (photon a1 and photon a2) and B (photon b) before teleportation. To verify this, the teleported ququart state of photon b is then analyzed by the measurement setup consisting of BD2, its surrounding waveplates, the polarization beamsplitter (PBS) and the single-photon detector D3 (See Methods: State analysis of a photonic ququart state). We measure the fidelity of the teleported state, $F = \text{Tr}(\rho|\psi\rangle\langle\psi|)$, which is defined as the overlap between the ideal teleported state ($|\psi\rangle$) and the measured density matrix (ρ). The verification of the quantum state transfer results is

based on fourfold coincidence detection which in our experiment occur with a rate of 0.22 Hz. In each setting, the typical data collection time is 10 minutes, which allows us to sufficiently suppress Poisson noise.

Figure 3a-i shows the general local quantum teleportation results of the nine different initial states on specific bases, from which the fidelities can be directly extracted. For each of the nine initial states $|\psi_1\rangle_{AB}$ to $|\psi_9\rangle_{AB}$, the fidelity of the final state of ququart B is, in numerical sequence: 0.8018 ± 0.0271 , 0.7220 ± 0.0289 , 0.6997 ± 0.0241 , 0.8772 ± 0.0217 , 0.7897 ± 0.0257 , 0.8080 ± 0.0249 , 0.8770 ± 0.0130 , 0.8431 ± 0.0134 , and 0.9171 ± 0.0138 , which are summarized in Fig. 3j.

The reported data are raw data without any background subtraction, and the main error are due to double pair emission, imperfection in preparation of the initial states, and the non-ideal interference at the PPBS and BD2. Despite the experimental noise, the measured fidelities of the quantum states are all well above the classical limit $2/3$, defined as the optimal state-estimation fidelity on a single copy of a one-qubit system [31]. These results prove the successful realization of general local quantum teleportation.

Conclusions and outlook—In summary, we have experimentally teleported an unknown qubit to a photon preloaded with one qubit of quantum information, demonstrating that quantum information can be freely transferred from one object to another, even if the target object contains pre-existing quantum information. Although the present experiment is realized in the linear optical architecture, our protocol itself is not limited to optical system and can be applied to other quantum systems such as trapped atoms [9], ions [10, 11], and electrons [12].

Our teleportation experiment have merged the quantum information previously distributed over three photons into a single photon, indicating that quantum information is independent of its carriers and can be freely moved around between different objects. Following this train of thought, an interesting next step would be realizing an opposite operation “partial teleportation”, namely transferring part of quantum information from one object to another object. An experiment is currently being conducted by the authors to demonstrate this “partial teleportation” operation [32].

Besides the fundamental interest, the methods developed in this work on realizing qubit-qudit quantum gates, may open up new possibilities in quantum technologies. Our approach can be easily extended to the high-dimensional case, i.e., transferring a qubit to a particle preloaded with a qudit (See Methods: Merge operation). Such operations have the potential to simplify the realization of complicated multi-qubit gates (See Methods: Simplifying multi-qubit gates) and find applications in quantum computation and quantum simulation.

* These authors contributed equally

† Electronic address: zhouxq8@mail.sysu.edu.cn

- [1] Bennett, C. H. *et al.* Teleporting an unknown quantum state via dual classical and einstein-podolsky-rosen channels. Phys. Rev. Lett. **70**, 1895-1899 (1993).
- [2] Ekert, A. K. Quantum cryptography based on bell's theorem. Phys. Rev. Lett. **67**, 661-663 (1991)
- [3] Kimble, H. J. The quantum internet. Nature **453**, 1023 (2008).
- [4] Raussendorf, R., *et al.* A one-way quantum computer. Phys. Rev. Lett. **86**, 5188-5191 (2001).
- [5] Raussendorf, R., *et al.* Measurement-based quantum computation on cluster states. Phys. Rev. A **68**, 022312 (2003).
- [6] Walther, P. *et al.* Experimental one-way quantum computing. Nature **434**, 169-176 (2005).
- [7] Bouwmeester, Dik, *et al.* Experimental quantum teleportation. Nature **390** (6660), 575-579 (1997).
- [8] Furusawa, Akira, *et al.* Unconditional quantum teleportation. science **282** (5389), 706-709 (1998).
- [9] Bao, Xiao-Hui, *et al.* Quantum teleportation between remote atomic-ensemble quantum memories. Proceedings of the National Academy of Sciences **109** (50), 20347-20351 (2012).
- [10] Riebe, Mark, *et al.* Deterministic quantum teleportation with atoms. Nature **429** (6993), 734-737 (2004).
- [11] Barrett, M. D., *et al.* Deterministic quantum teleportation of atomic qubits. Nature **429** (6993), 737-739 (2004).
- [12] Qiao, H., *et al.* Conditional teleportation of quantum-dot spin states. Nature communications **11** (1), 1-9 (2020).
- [13] Pfaff, W., *et al.* Unconditional quantum teleportation between distant solid-state quantum bits. Science **345** (6196), 532-535 (2014).
- [14] Steffen, Lars, *et al.* Deterministic quantum teleportation with feed-forward in a solid state system. Nature **500** (7462), 319-322 (2013).
- [15] Zhao, Z., *et al.* Experimental demonstration of five-photon entanglement and open-destination teleportation. Nature **430** (6995), 54-58 (2004).
- [16] Barasinski, A., *et al.* Demonstration of controlled quantum teleportation for discrete variables on linear optical devices. Phys. Rev. Lett. **122** (17), 170501 (2019).
- [17] Zhang, Q., *et al.* Experimental quantum teleportation of a two-qubit composite system. Nature Physics **2**(10), 678-682 (2006).
- [18] Hu, X., *et al.* Experimental multi-level quantum teleportation. arXiv preprint arXiv:1904.12249 (2019).
- [19] Luo, Y., *et al.* Quantum Teleportation in High Dimensions. Phys. Rev. Lett. **123** (7), 070505 (2019).
- [20] Wang, X., *et al.* Quantum teleportation of multiple degrees of freedom of a single photon. Nature **518** (7540), 516-519 (2015).

- [21] Zhou, X., Leung, D. W., and Chuang, I. L. Methodology for quantum logic gate construction. *Physical Review A*, **62**(5), 052316 (2000).
- [22] Nielsen, M. A. Cluster-state quantum computation. *Reports on Mathematical Physics*, **57**(1), 147-161 (2006).
- [23] Nielsen, M. A. and Chuang, I. L. *Quantum Computation and Quantum Information* (Cambridge Univ. Press, 2000)
- [24] Barenco, A., *et al.* Elementary gates for quantum computation. *Phys. Rev. A* **52** (5), 3457 (1995)
- [25] Vidal, G., *et al.* Universal quantum circuit for two-qubit transformations with three controlled-NOT gates. *Phys. Rev. A* **69** (1), 010301 (2004).
- [26] O'Brien, J. L., *et al.* Demonstration of an all-optical quantum controlled-NOT gate. *Nature* **426** (6964), 264-267 (2003).
- [27] Chou, K. S., *et al.* Deterministic teleportation of a quantum gate between two logical qubits. *Nature* **561** (7723), 368-373 (2018).
- [28] Fedorov, A., *et al.* Implementation of a Toffoli gate with superconducting circuits. *Nature* **481** (7380), 170-172 (2012).
- [29] Reed, M. D., *et al.* Realization of three-qubit quantum error correction with superconducting circuits. *Nature* **482** (7385), 382-385 (2012).
- [30] Please see supplementary information.
- [31] Massar, S., *et al.* Optimal Extraction of Information from Finite Quantum Ensembles, *Phys. Rev. Lett.* **74** (8), 1259-1263 (1995).
- [32] Feng, T. *et al.* Quantum partial teleportation (in preparation)
- [33] Ralph, T. C., *et al.* A. Efficient Toffoli gates using qudits. *Phys. Rev. A* **75**, 022313 (2007)
- [34] Lanyon, B. P., *et al.* Simplifying quantum logic using higher-dimensional Hilbert spaces. *Nat. Physics* **5**(2),134-140 (2009).

DATA AVAILABILITY

The data that support this study are available from the corresponding author upon reasonable request.

ACKNOWLEDGEMENTS

This work was supported by the National Key Research and Development Program of China (2017YFA0305200, 2016YFA0301300), the Key Research and Development Program of Guangdong Province (2018B030329001, 2018B030325001) and the National Natural Science Foundation of China (Grant No.61974168).

AUTHOR CONTRIBUTIONS

X.Z. conceived the idea for and designed the research; X.Z. and T.F. performed the theoretical analysis; T.F., Q.X., L.Z., M.L. and W.Z. performed the experiment; X.Z. and T.F. wrote the paper with input from all authors; T.F., Q.X. and L.Z. contributed equally; X.Z. supervised the whole project.

COMPETING INTERESTS

The authors declare that there are no competing interests.

METHODS

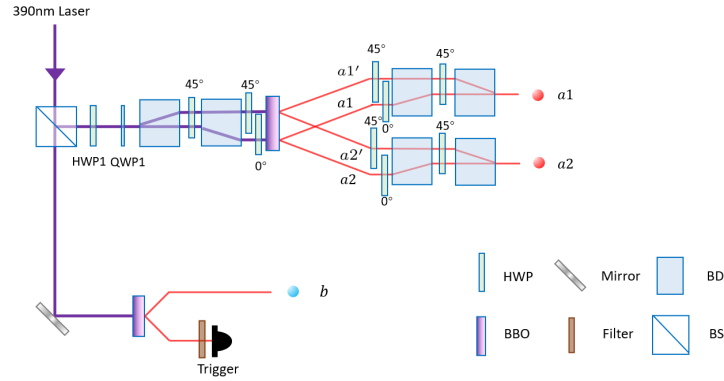


Fig. S1. Experimental setup for generating two photon pairs.

Generating two photon pairs. For the sake of simplicity, in Fig. 2b of the main text, we only show a simplified version of the spontaneous parametric down-conversion (SPDC) sources. Figure S1 shows the detailed experimental setup for generating two photon pairs. An ultraviolet pulse laser centered at 390nm is split into two parts, which are used to generate two SPDC photon pairs. The lower part of the laser directly pumps a BBO crystal to generate a pair of photons in the state $|V_b\rangle|H_t\rangle$ via beam-like type-II SPDC, where photon t is used for trigger. The upper part of the laser goes through HWP1 and QWP1 to prepare its polarization at $\alpha|H\rangle + \beta|V\rangle$. It then passes through an arrangement of two beam displacers (BDs) and HWPs to separate the laser into two beams by 4 mm apart (such configuration was first adopted by H.-S. Zhong et al. in [5]). The two beams then focus on a BBO crystal to generate two photon pairs in the states $|V_{a1}\rangle|H_{a2}\rangle$ and $|V_{a1'}\rangle|H_{a2'}\rangle$ via beamlike type-II SPDC, where the subscripts denote

the spatial modes. $|V_{a1}\rangle|H_{a2}\rangle$ and $|V_{a1'}\rangle|H_{a2'}\rangle$ are then rotated using HWPs to $|H_{a1}\rangle|H_{a2}\rangle$ and $|V_{a1'}\rangle|V_{a2'}\rangle$, respectively. Photon pairs of $|H_{a1}\rangle|H_{a2}\rangle$ and $|V_{a1'}\rangle|V_{a2'}\rangle$ are then combined into same spatial modes using two BDs. After tilting the two BDs to finely tune the relative phase between the two components, the two photons a1 and a2 are prepared into $\alpha|H\rangle_{a1}|H\rangle_{a2} + \beta|V\rangle_{a1}|V\rangle_{a2}$, which is the desired quantum state of system A.

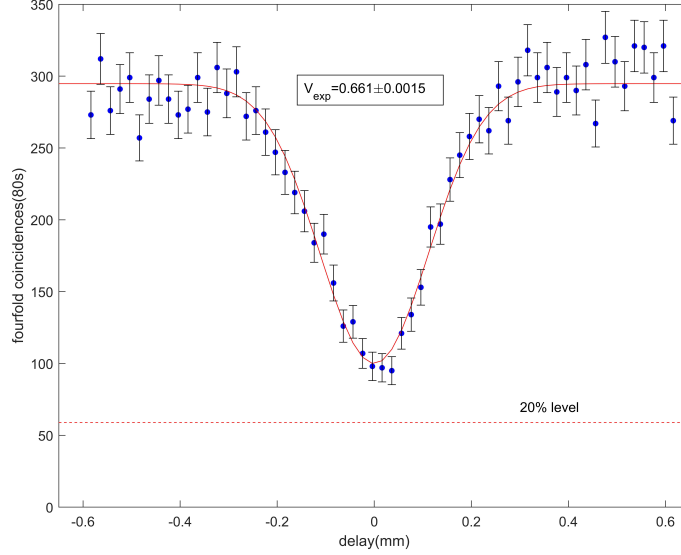


Fig. S2. HOM interference at the PPBS for a $|HH\rangle$ input. In case of perfect interference, the count rate should drop down to 20%, leading to a theoretically achievable dip visibility of 80%.

Two-photon interference on a PPBS. The PPBS implements the quantum phase gate by reflecting vertically polarized light perfectly and reflecting (transmitting) 1/3 (2/3) of horizontally polarized light. To realize a perfect quantum gate with the PPBS, the input photons on the PPBS need to be indistinguishable to each other. To evaluate the indistinguishability of the input photons, a two-photon Hong-Ou-Mandel (HOM) interference on the PPBS need to be measured. For large delay, the two photons are completely distinguishable due to their time of arrival. The probability to get a coincidence from a $|HH\rangle$ input is then 5/9. In case of perfectly indistinguishable photons at zero delay, the probability drops to 1/9. From the above considerations, the theoretical dip visibility $V_{th} = 80\%$ is obtained, which is defined via $V = (c_{\infty} - c_0)/c_0$, where c_0 is the count rate at zero delay and c_{∞} is the count rate for large delay. As shown in Fig. S2, the HOM interference is experimentally measured and a dip visibility of $V_{exp} = 0.661 \pm 0.0015$ is obtained, where the error bar is calculated from the Poissonian counting statistics of the detection events. The overlap quality $Q = V_{exp}/V_{th} = 0.826 \pm 0.0019$ indicates that about 17.4% of the detected photon pairs are distinguishable.

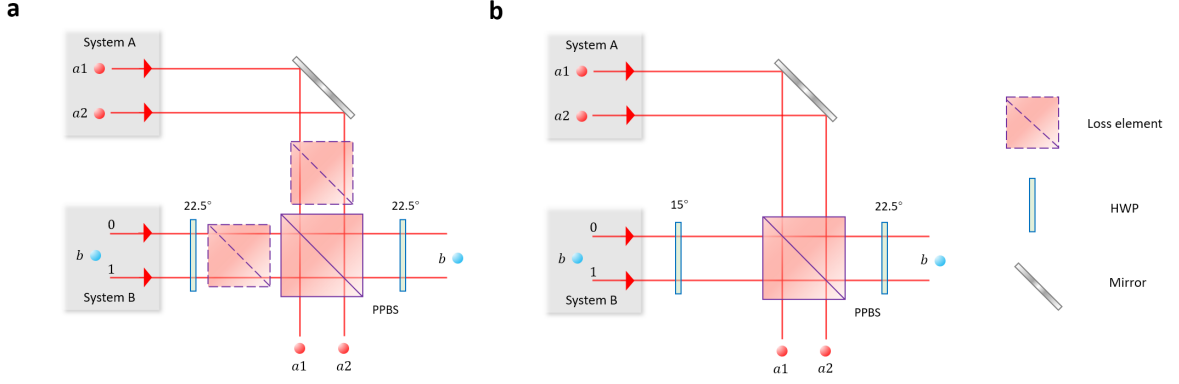


Fig. S3. CX_4 gate with linear optics. **a**, The standard optical CX_4 gate. **b**, The simplified optical CX_4 gate.

Implementation of CX_4 gate using linear optics. As described in the main text, an optical CX_4 gate between system A (photons a_1 and a_2) and system B (photon b) can be implemented with a setup as shown in Fig. S3a. Photons a_1 and a_2 encode the control qubit and its initial state is $\alpha|\mathbf{0}\rangle_A + \beta|\mathbf{1}\rangle_A = \alpha|H\rangle_{a_1}|H\rangle_{a_2} + \beta|V\rangle_{a_1}|V\rangle_{a_2}$. Photon b encodes the target ququart and its initial state is $\gamma|\mathbf{0}\rangle_B + \delta|\mathbf{1}\rangle_B = \gamma|H0\rangle_b + \delta|H1\rangle_b$. After passing through the loss elements that transmit horizontally polarized light perfectly and transmit $1/3$ of vertically polarized light, photon a_1 (a_2) and photon b in the upper (lower) mode are superposed on the PPBS. The PPBS, the loss elements and the two surrounding HWPs at 22.5° together implement a polarization CNOT operation on the input photons [3, 6, 7]. Such optical circuit can thus realize the following transformations

$$|H\rangle_{a_1}|H\rangle_{a_2} \otimes |H0\rangle_b \longrightarrow |H\rangle_{a_1}|H\rangle_{a_2} \otimes |H0\rangle_b$$

$$|H\rangle_{a_1}|H\rangle_{a_2} \otimes |H1\rangle_b \longrightarrow |H\rangle_{a_1}|H\rangle_{a_2} \otimes |H1\rangle_b$$

$$|V\rangle_{a_1}|V\rangle_{a_2} \otimes |H0\rangle_b \longrightarrow |V\rangle_{a_1}|V\rangle_{a_2} \otimes |V0\rangle_b$$

$$|V\rangle_{a_1}|V\rangle_{a_2} \otimes |H1\rangle_b \longrightarrow |V\rangle_{a_1}|V\rangle_{a_2} \otimes |V1\rangle_b.$$

As a result, after passing through this optical circuit, the initial input state

$$\begin{aligned} & (\alpha|\mathbf{0}\rangle_A + \beta|\mathbf{1}\rangle_A) \otimes (\gamma|\mathbf{0}\rangle_B + \delta|\mathbf{1}\rangle_B) \\ &= (\alpha|H\rangle_{a_1}|H\rangle_{a_2} + \beta|V\rangle_{a_1}|V\rangle_{a_2}) \otimes (\gamma|H0\rangle_b + \delta|H1\rangle_b) \end{aligned}$$

would become

$$\begin{aligned}
& \alpha|H\rangle_{a1}|H\rangle_{a2} \otimes (\gamma|H0\rangle_b + \delta|H1\rangle_b) \\
& + \beta|V\rangle_{a1}|V\rangle_{a2} \otimes (\gamma|V0\rangle_b + \delta|V1\rangle_b) \\
& = \alpha|\mathbf{0}\rangle_A \otimes (\gamma|\mathbf{0}\rangle_B + \delta|\mathbf{1}\rangle_B) + \beta|\mathbf{1}\rangle_A \otimes (\gamma|\mathbf{2}\rangle_B + \delta|\mathbf{3}\rangle_B),
\end{aligned}$$

which is exactly the desired output state of a CX_4 gate. The above optical CX_4 gate operates with a success probability of $1/27$. In practice, to combat low count rates, we adopt the method proposed in reference [3] to simplify the implementation of the optical CX_4 gate. The simplified experimental setup is shown in Fig. S3b. We achieve correct balance by removing the loss elements and pre-biasing the input polarization states during gate characterization. The initial state of photons a1 and a2 is now prepared at $\frac{\alpha}{\sqrt{|\alpha|^2 + \frac{1}{9}|\beta|^2}}|H\rangle_{a1}|H\rangle_{a2} + \frac{\beta/3}{\sqrt{|\alpha|^2 + \frac{1}{9}|\beta|^2}}|V\rangle_{a1}|V\rangle_{a2}$ instead of $\alpha|H\rangle_{a1}|H\rangle_{a2} + \beta|V\rangle_{a1}|V\rangle_{a2}$. The HWP applied on photon b before entering the PPBS is now set at 15° , thus converting photon b to the state $\frac{\sqrt{3}}{2}(\gamma|H0\rangle + \delta|H1\rangle) + \frac{1}{2}(\gamma|V0\rangle + \delta|V1\rangle)$ instead of $\frac{1}{\sqrt{2}}(\gamma|H0\rangle + \delta|H1\rangle) + \frac{1}{\sqrt{2}}(\gamma|V0\rangle + \delta|V1\rangle)$, which is the case if the HWP is set at 22.5° .

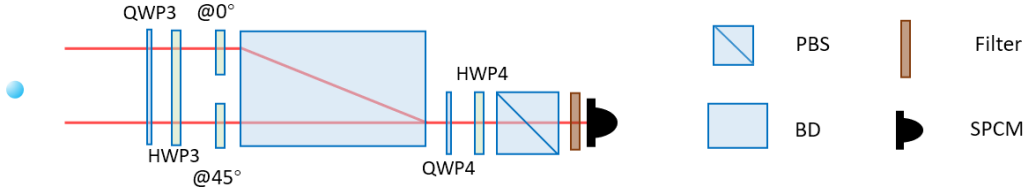


Fig. S4. State analyzer for a single-photon ququart state with both polarization and spatial degrees of freedom.

State analysis of a photonic ququart state. A photon with both polarization and spatial degrees of freedom (DOFs) can encode a ququart state. To fully characterize such state, one needs to perform projective measurement onto various different ququart states. To fulfill this task, we build a ququart state analyzer as shown in Fig. S4, which can project the input ququart to any state in the form of $(a|H\rangle + b|V\rangle) \otimes (c|0\rangle + d|1\rangle)$. This setup works as follows: Suppose the input ququart state is $(a|H\rangle + b|V\rangle) \otimes (c|0\rangle + d|1\rangle)$. After passing through QWP3 and HWP3, which are used to convert $a|H\rangle + b|V\rangle$ to $|H\rangle$, the ququart state becomes $|H\rangle \otimes (c|0\rangle + d|1\rangle)$. The subsequent two HWPs (one at 45° and the other at 0°) and the BD are used to convert $|H\rangle \otimes (c|0\rangle + d|1\rangle)$ to $c|H\rangle + d|V\rangle$, which is now a polarization qubit state. QWP4 and HWP4 are then used to convert $c|H\rangle + d|V\rangle$ to $|H\rangle$, which can pass through the PBS and get detected by the SPD. As a result, for any input ququart state, only its $(a|H\rangle + b|V\rangle) \otimes (c|0\rangle + d|1\rangle)$

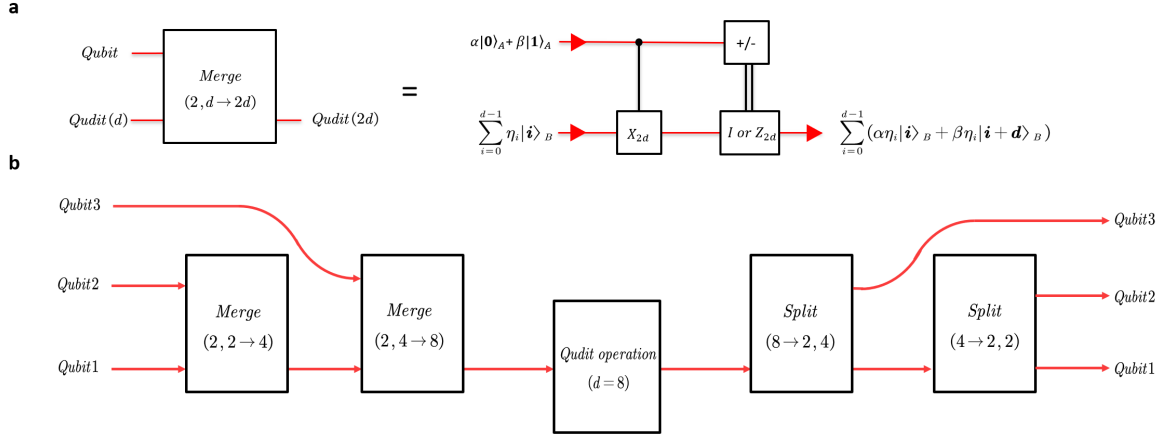


Fig. S5. **a**, The Merge operation. The quantum circuit for merging the quantum information of a qubit and a d-dimensional qudit into a 2d-dimensional qudit. **b**, Implementing a three-qubit quantum gate.

component can pass through the setup described above, which effectively realize the desired projective measurement. By changing the parameters a, b, c and d, this state analyzer can be used to perform a full state tomography on the input ququart state.

Merge operation. The scheme of general local quantum teleportation can be extended to the higher dimensional case, i.e., transferring a qubit to a particle with a preloaded d-dimensional qudit. We call this operation of aggregating quantum information from two particles to one particle the Merge operation, and $\text{Merge}(2, d \rightarrow 2d)$ denotes the aggregation of quantum information of a qubit and a d-dimensional qudit to a 2d-dimensional qudit. The quantum circuit to implement $\text{Merge}(2, d \rightarrow 2d)$ is shown in Fig. S5a, where the initial state of system A is $\alpha|0\rangle_A + \beta|1\rangle_A$ and the initial state of system B is $\sum_{i=0}^{d-1} \eta_i |\mathbf{i}\rangle$, which is a d-dimensional qudit. A controlled- X_{2d} (CX_{2d}) gate is applied to A and B, where X_{2d} is a 2d-dimensional unitary gate defined as $X_{2d} = \sum_{\mathbf{k}=0}^{d-1} (|\mathbf{k}\rangle\langle \mathbf{k} + \mathbf{d}| + |\mathbf{k} + \mathbf{d}\rangle\langle \mathbf{k}|)$, which swaps $|\mathbf{k}\rangle$ and $|\mathbf{k} + \mathbf{d}\rangle$ for k in the range of 0 to d-1, expanding the state space of system B from d to 2d dimensions. The state of A and B is thus converted from

$$\begin{aligned}
 & (\alpha|0\rangle + \beta|1\rangle) \otimes \sum_{i=0}^{d-1} \eta_i |\mathbf{i}\rangle \\
 &= \sum_{i=0}^{d-1} (\alpha\eta_i |0\rangle_A |\mathbf{i}\rangle_B + \beta\eta_i |1\rangle_A |\mathbf{i}\rangle_B)
 \end{aligned} \tag{3}$$

to

$$\begin{aligned}
& \sum_{i=0}^{d-1} (\alpha\eta_i |\mathbf{0}\rangle_A |\mathbf{i}\rangle_B + \beta\eta_i |\mathbf{1}\rangle_A |\mathbf{i} + \mathbf{d}\rangle_B) \\
&= |+\rangle_A \otimes \sum_{i=0}^{d-1} (\alpha\eta_i |\mathbf{i}\rangle_B + \beta\eta_i |\mathbf{i} + \mathbf{d}\rangle_B) \\
&+ |-\rangle_B \otimes \sum_{i=0}^{d-1} (\alpha\eta_i |\mathbf{i}\rangle_B - \beta\eta_i |\mathbf{i} + \mathbf{d}\rangle_B).
\end{aligned}$$

After measuring A in the $|\pm\rangle$ basis and forwarding the outcome to B, a 2d-dimensional unitary operation (I_{2d} or Z_{2d}) is applied on B conditioned on the outcome and thus converts its state to

$$\sum_{i=0}^{d-1} (\alpha\eta_i |\mathbf{i}\rangle_B + \beta\eta_i |\mathbf{i} + \mathbf{d}\rangle_B), \quad (4)$$

where

$$Z_{2d} = I_{2d} - 2 \sum_{k=0}^{d-1} |\mathbf{k} + \mathbf{d}\rangle \langle \mathbf{k} + \mathbf{d}|.$$

By comparing Eq. (4) and Eq. (3), one can see that the two quantum states have exactly the same form except for the difference in the state basis, which means that the quantum information originally stored in A and B has been merged into B.

Simplifying multi-qubit gates. In various quantum information applications, including quantum computation and quantum simulation, multi-qubit quantum gates are widely used. Theoretically, multi-qubit quantum gates can be decomposed into two-qubit CNOT gates and single-qubit quantum gates for implementation, but in practice, such decomposition can be quite complex and consumes a lot of resources experimentally. Here we propose a method to simplify the implementation of multi-qubit quantum gates by using quantum state transfer. This approach essentially transforms an arbitrary n-qubit quantum gate operation into a unitary transform on a 2^n -dimensional qudit, which is simpler to implement in certain circumstances. For example, for a path-encoded 2^n -dimensional photon, when n is not very large, an arbitrary $2^n \times 2^n$ qudit unitary transform can be readily implemented using the Reck scheme [8, 9]. We present below our method using a 3-qubit quantum gate as an example. Specifically, the method can be divided into three steps. (i) The quantum information of the three input qubits is converged to a single particle, which can be achieved by two Merge operations. As shown in Fig. 9c, a ququart is obtained by a Merge(2, 2→4) operation acting on qubit 2 and qubit 1. Then a Merge(2, 4→8) operation acts on qubit 3 and this ququart to obtain a qudit (d=8), which contains the quantum information of the input three qubits. (ii) The qudit is then subjected to a 8×8 unitary transformation, which has the same mathematical form as the matrix of the 3-qubit quantum

gate expanded in the computational basis. (iii) The quantum information of this qudit is then distributed to three particles, which can be achieved by two Split operations which are the inverse operation of Merge operations. The 8-dimensional qudit is split by a Split($8 \rightarrow 2, 4$) operation to get a qubit and a ququart, and this ququart is then split by a Split($4 \rightarrow 2, 2$) operation to finally get 3 qubits at the output, thus completing the 3-qubit quantum gate. For an arbitrary n-qubit quantum gate, it is often simpler and more resource-efficient to use our method than the traditional decomposition of n-qubit quantum gates into CNOT gates and single-qubit quantum gates, as long as n is not very large, i.e., the 2^n -dimensional qudit can be easily unitary-transformed.

* These authors contributed equally

† Electronic address: zhouxq8@mail.sysu.edu.cn

- [1] H. S. Zhong, Y. Li, W. Li, *et al.* 12-photon entanglement and scalable scattershot boson sampling with optimal entangled-photon pairs from parametric down-conversion. *Phys. Rev. Lett.* **121**(25), 250505. (2018)
- [2] Langford, N. K. *et al.* Demonstration of a simple entangling optical gate and its use in Bell-state analysis. *Phys. Rev. Lett.* **95**, 210504 (2005)
- [3] Okamoto, R., *et al.* Demonstration of an optical quantum controlled-NOT gate without path interference. *Phys. Rev. Lett.* **95**, 210506. (2005)
- [4] Kiesel, N. *et al.* Linear optics controlled-phase gate made simple. *Phys. Rev. Lett.* **95**, 210505 (2005)
- [5] Zhong, H. S. *et al.* 12-photon entanglement and scalable scattershot boson sampling with optimal entangled-photon pairs from parametric down-conversion. *Phys. Rev. Lett.* **121** (25), 250505 (2018).
- [6] Langford, N. K. *et al.* Demonstration of a simple entangling optical gate and its use in Bell-state analysis. *Phys. Rev. Lett.* **95** (21), 210504 (2005).
- [7] Kiesel, N. *et al.* Linear optics controlled-phase gate made simple. *Phys. Rev. Lett.* **95** (21), 210505 (2005).
- [8] Reck, M. *et al.* Experimental realization of any discrete unitary operator. *Phys. Rev. Lett.* **73** (1) 58–61 (1994).
- [9] Clements, W. R. *et al.* Optimal design for universal multiport interferometers. *Optica* **3** (12), 1460 (2016).